

# Pion interferometry with pion–source-medium interactions

M.-C. Chu<sup>1</sup>, S. Gardner<sup>2</sup>, T. Matsui<sup>2,3</sup>, and R. Seki<sup>1,4</sup>

<sup>1</sup> *W. K. Kellogg Radiation Laboratory, California Institute of Technology  
Pasadena, California 91125*

<sup>2</sup> *Nuclear Theory Center, Indiana University, Bloomington, Indiana 47408*

<sup>3</sup> *Yukawa Institute for Theoretical Physics, Kyoto University, Kyoto 606, Japan*

<sup>4</sup> *Department of Physics and Astronomy, California State University  
Northridge, California 91330*

(October 23, 2018)

## Abstract

An extended pion source, which can be temporarily created by a high energy nuclear collision, will also absorb and distort the outgoing pions. We discuss how this effect alters the interferometric pattern of the two-pion momentum correlation function. In particular, we show that the two-pion correlation function decreases rapidly when the opening angle between the pions increases. The opening-angle dependence should serve as a new means of obtaining information about the pion source in the analysis of experimental data.

PACS numbers: 25.75.+r, 13.60.Le, 13.75.Gx

## I. INTRODUCTION

Hanbury-Brown-Twiss interferometry of identical particles emitted from a chaotic source has long been used to infer the spatial and temporal characteristics of that source [1,2,3,4,5,6,7,8]. Although originally conceived in astronomy to the end of extracting stellar radii [1], the technique has found extensive application as a diagnostic tool in heavy-ion collisions [5,6,7,8,9]. In most practical applications, the outgoing pions are assumed to suffer only weak final-state interactions. For instance, the interaction between the two detected pions is usually neglected, and a simple plane wave solution is used to calculate the two pion momentum correlation function, although in the case of charged pions, it is multiplied by the Gamow factor to correct for their long-range Coulomb force.

In this paper, we discuss another type of final-state interaction, wherein each pion suffers in its exit from the source region. Namely, *the interaction of the pions with the “source” itself*. Since a pion source also absorbs and distorts pions, a source with finite extent in space and time will alter the outgoing pion waves in the source region. In particular, if the pion source is a droplet of “quark-gluon plasma,” it may be regarded as a black-body of pions — and of all other hadrons — so that it casts its shadow on the paths of the outgoing pions emitted from the plasma surface. In a classical picture, this effect may be taken into account by introducing a strong correlation between the pion momentum and its emission points, so that the pions are emitted only in outward directions, an effect similar to that caused by collective flow [10,11]. Pions may also interact in a dense pion medium via  $\rho$  or  $\omega$  resonance formation, for example, and change the effective source size [12]. One can also include baryon resonances explicitly in the pion source [13]. Yet there is a fundamentally more important effect which arises due to the quantum mechanical nature of interferometry: *the distortion of the interference pattern generated by the pion–source–medium interaction*.

Here we study the pion correlation function in the presence of pion–source–medium interactions, as represented by a local optical potential, within the eikonal approximation. We calculate the distortion of the pion wave function explicitly, thereby allowing for a direct investigation of the quantum mechanical interference effects. We show that both the real and the imaginary parts of the optical potential give rise to non-trivial modifications: the former induces additional interference effects, whereas the latter leads to a suppression of the correlation as the opening angle between the pions increases. We demonstrate that the opening angle-averaged correlation function acquires a non-Gaussian shape due to these interactions, even if the source distribution is Gaussian.

## II. BASIC PRINCIPLES

Before proceeding to include the final-state interactions, we first review the basic principles of two-particle interferometry. Such a description is easily found in the literature; we present it here to clarify its usual assumptions, as well as the manner in which we include pion–source–medium interactions.

In essence, two particle interferometry results from a constructive — or destructive — interference of the two amplitudes for the emission of two identical bosons — or fermions — from two independent sources. Suppose that there are  $N$  such independent sources, localized at the space-time points  $x_i$  ( $i = 1, \dots, N$ ), and that the emitted particles do not interact with

each other after their creation. Let  $\varphi_{\mathbf{k}}(x_i)$  be the amplitude that a particle with momentum  $\mathbf{k}$  is emitted from a source at  $x_i$ . Then the pair amplitude  $\Psi_{\mathbf{k}_1\mathbf{k}_2}(x_i, x_j)$  that two particles are created by the source at  $x_i$  and  $x_j$  and are detected later with momenta  $\mathbf{k}_1$  and  $\mathbf{k}_2$  is written in a product *Ansatz* as

$$\Psi_{\mathbf{k}_1\mathbf{k}_2}(x_i, x_j) = \frac{1}{\sqrt{2}} e^{i(\delta_i + \delta_j)} [\varphi_{\mathbf{k}_1}(x_i)\varphi_{\mathbf{k}_2}(x_j) \pm \varphi_{\mathbf{k}_1}(x_j)\varphi_{\mathbf{k}_2}(x_i)] . \quad (1)$$

We have taken out the overall phase factors associated with the arbitrary phase of each single particle amplitude, and since the detected particles are on shell, we can label the pair amplitude with just the three-momenta  $\mathbf{k}_1, \mathbf{k}_2$ . The first term is the amplitude that the particle of momentum  $\mathbf{k}_1$  is produced at  $x_i$  with the particle of momentum  $\mathbf{k}_2$  produced at  $x_j$ . The second term is needed to ensure the proper symmetry of the total amplitude with respect to exchange of the particle coordinates — (+) for boson pairs and (−) for fermion pairs. The probability of observing a particle with momentum  $\mathbf{k}$  is given by

$$P_1(\mathbf{k}) = \frac{1}{N} \left\langle \left| \sum_i e^{i\delta_i} \varphi_{\mathbf{k}}(x_i) \right|^2 \right\rangle , \quad (2)$$

whereas the joint probability of finding two particles with momenta  $\mathbf{k}_1$  and  $\mathbf{k}_2$  is

$$P_2(\mathbf{k}_1, \mathbf{k}_2) = \frac{1}{N(N-1)} \left\langle \left| \sum_{i \neq j} \Psi_{\mathbf{k}_1\mathbf{k}_2}(x_i, x_j) \right|^2 \right\rangle . \quad (3)$$

Note that  $\langle \dots \rangle$  indicates an average over the source distribution. The two-particle momentum correlation function is defined by

$$C_2(\mathbf{k}_1, \mathbf{k}_2) \equiv \frac{P_2(\mathbf{k}_1, \mathbf{k}_2)}{P_1(\mathbf{k}_1)P_1(\mathbf{k}_2)} . \quad (4)$$

With a few more assumptions, to be summarized below, the momentum correlation function is related directly to the Fourier transform of the source distribution,  $\tilde{\rho}_{\tilde{q}} \equiv \int d^4x \rho(x) e^{i\tilde{q}x}$ . Namely,

$$C_2(\mathbf{k}_1, \mathbf{k}_2) = 1 \pm \left[ |\tilde{\rho}_{\tilde{q}}|^2 / |\tilde{\rho}_{\tilde{q}=0}|^2 \right] , \quad (5)$$

where  $\tilde{q} \equiv (E_1 - E_2, \mathbf{k}_1 - \mathbf{k}_2)$  is the relative four-momentum. Hence Eq. (5) predicts that

$$C_2(\mathbf{k}_1, \mathbf{k}_2) \rightarrow 2(0) \quad \text{as} \quad \tilde{q} \rightarrow 0 \quad (6)$$

for boson (fermion) pairs, whereas  $C_2 \rightarrow 1$  as  $\tilde{q} \rightarrow \infty$  in both cases.

There are three assumptions, besides the *Ansatz* in Eq. (1), involved in deriving the above from Eq. (4).

1. The relative phases of particles created at different locations are incoherent — the phase average is random.
2. There are no correlations in the source distribution.

3. The particles do not interact after their emission.

The first assumption is the most important of all: it allows us to write the probability distribution in terms of an *incoherent sum* of the individual probabilities. That is,

$$P_1(\mathbf{k}) = \frac{1}{N} \langle \sum_i |\varphi_{\mathbf{k}_1}(x_i)|^2 \rangle = \int d^4x \rho(x) |\varphi_{\mathbf{k}_1}(x)|^2, \quad (7)$$

$$\begin{aligned} P_2(\mathbf{k}_1, \mathbf{k}_2) &= \frac{1}{N(N-1)} \langle \sum_{i,j} |\Psi_{\mathbf{k}_1\mathbf{k}_2}(x_i, x_j)|^2 \rangle \\ &= \int d^4x_1 d^4x_2 \rho_2(x_1, x_2) |\Psi_{\mathbf{k}_1\mathbf{k}_2}(x_1, x_2)|^2, \end{aligned} \quad (8)$$

where the averages over the  $N$  point sources are replaced by integrals over smooth distributions. All the interference terms containing the relative phase factor  $e^{i(\delta_i - \delta_j)}$  drop out when averaged over the random phases  $\delta_i$ . Note that the two terms in the bracket of Eq. (1) have a definite relative phase, so that their interference survives the random phase averaging. The second assumption allows us to replace the two-particle source distribution  $\rho_2(x_1, x_2)$  by the product of the single particle source distributions:

$$\rho_2(x_1, x_2) = \rho(x_1)\rho(x_2). \quad (9)$$

This factorization does not hold in the presence of fine structure in the source, for example, in the multidroplet model of the mixed phase [14]. Lastly, by the third assumption, the single particle amplitude  $\varphi_{\mathbf{k}}(x)$  is given as a solution of the free Klein-Gordon or Dirac equation, as appropriate:

$$\varphi_{\mathbf{k}}(x) = c_{\mathbf{k}} e^{ik \cdot x}. \quad (10)$$

Note that the normalization factors  $c_{\mathbf{k}}$  cancel out in the correlation function of Eq. (4).

Finally, these assumptions lead to the expression [5,6,7]

$$C_2(\mathbf{k}_1, \mathbf{k}_2) = \frac{\int d^4x_1 d^4x_2 \rho(x_1)\rho(x_2) |\Psi_{\mathbf{k}_1\mathbf{k}_2}(x_1, x_2)|^2}{\int d^4x_1 \rho(x_1) |\varphi_{\mathbf{k}_1}(x_1)|^2 \int d^4x_2 \rho(x_2) |\varphi_{\mathbf{k}_2}(x_2)|^2}, \quad (11)$$

where

$$\Psi_{\mathbf{k}_1\mathbf{k}_2}(x_1, x_2) = \frac{1}{\sqrt{2}} [\varphi_{\mathbf{k}_1}(x_1)\varphi_{\mathbf{k}_2}(x_2) \pm \varphi_{\mathbf{k}_2}(x_1)\varphi_{\mathbf{k}_1}(x_2)]. \quad (12)$$

### III. INCLUSION OF PION-SOURCE-MEDIUM INTERACTIONS

We now turn our discussion to the modification of the correlation function due to the inclusion of final-state interactions. In principle, there are two types of final-state interactions to be considered: the mutual interaction between the detected pions, and the interaction of the pions with the rest of the system. The former effect may be included by solving the Bethe-Salpeter equation or the Schrödinger equation for the two-body wave function [5,6].

Here we examine the latter effect, the medium modification [6,15]. We incorporate it by adding a self-energy term to the Klein-Gordon equation:

$$\left(\square + m^2 + 2mU(x)\right) \varphi_k(x) = 0 . \quad (13)$$

We have assumed that  $U(x)$  is a *local* optical potential. The heuristic derivation of Eq. (11) in Sec. II presumes that the pions do not interact after their emission. However, Eq. (11) still holds when a local one-body optical potential is included in the construction of  $\varphi_k(x)$  as long as  $U(x)$  does not support bound states or create real particle pairs [6].

Many of the complications associated with the heavy-ion reaction are lumped in the potential  $U(x)$ . For example, the pion source function  $\rho(x)$  appears explicitly in Eq. (11), but the dynamical response of the source to the interactions of the outgoing pion with the source medium does not. This response is contained in  $U(x)$  — it is the effective single-channel optical potential. The final sum over the unobserved hadronic states implicit in Eq. (11) can still be effected independently of the pion amplitudes in this picture. Furthermore, the initial state of the source function is also not identified, and for a given dynamical model description of the heavy-ion reaction, all allowed initial states must be averaged. We presume, for now, that this averaging can also be absorbed in  $U(x)$ .

The complexity of the optical potential is compounded by the time evolution of the source. For example, as the source expands, the relative momentum of the outgoing pion and of the source element with which it interacts changes in time and thereby alters the pion's interaction with the source. To illustrate this, consider an expanding source that consists merely of nucleons. The strength of the pion-nucleon interaction depends strongly on the relative momentum between the pion and the nucleon with which it interacts. Moreover, pion absorption by the source will depend on how two nucleons in the source are correlated in time. The complexity of  $U(x)$  can be reduced by constructing an explicit dynamical model of the heavy ion reaction, but simple physical insight into the effects of  $U(x)$  would be lost in such a task. Thus, we make the problem as simple as possible, in order to extract the essential physics that emerge as a consequence of the pion–source–medium interaction. To this end, we first choose to ignore the additional complications that arise from the time dependence of the source and consider merely a static pion interaction with the source medium. Note that Eq. (13) may then be interpreted as describing the time-reverse of the usual scattering process: the pion returns from infinity with momentum  $-\mathbf{k}$  and is inversely scattered by the optical potential  $U(x)$ . For pions with energies of a few hundred MeV,  $\varphi_{\mathbf{k}}(x)$  is given approximately by

$$\varphi_{\mathbf{k}}(x) = c_{\mathbf{k}} e^{ikx - \frac{im}{k} \int_z^\infty dz' U(x, y, z')} , \quad (14)$$

where  $(x, y, z)$  labels the pion production point. Note that  $z \equiv \hat{\mathbf{k}} \cdot \mathbf{r}$  and  $z'$  parametrizes the straight line path along  $\mathbf{k}$  from  $z$  to infinity. Equation (14) is the eikonal approximation and agrees well with elastic pion-nucleus scattering data in the energy regime we consider [16], when a realistic momentum-dependent potential is assumed. We will use the function  $\varphi_{\mathbf{k}}(x)$  in Eqs. (11) and (12) to include the final-state pion–source–medium interaction in the pion momentum correlation function.

Moreover, we choose a simple model for the pion–source–medium interaction — a complex constant multiplies the source density  $\rho$ :

$$\frac{m}{k} U(r) = (\sigma_R + i\sigma_I) \rho(r) . \quad (15)$$

In general,  $\sigma_R$  and  $\sigma_I$  may depend on the momentum of the pion with respect to the medium and on the temperature of the medium as well. We shall assume that  $\sigma_R$  and  $\sigma_I$  are simply constant, but we will examine a wide range of parameter values in order to probe the sensitivity of the pions' momentum correlation to this new effect. We can then write the distortion factor  $g(\mathbf{k}, \mathbf{r})$  as

$$g(\mathbf{k}, \mathbf{r}) = e^{-i(\sigma_R + i\sigma_I)t(\mathbf{k}, \mathbf{r})}, \quad (16)$$

where the thickness function  $t(\mathbf{k}, \mathbf{r}) \equiv \int_z^\infty dz' \rho(\mathbf{b}, z')$  is determined by the direction of the outgoing pion and its production point  $\mathbf{r}$ . The impact parameter  $\mathbf{b}$  is defined by  $\mathbf{r} - \mathbf{z}$ , where  $\mathbf{z} = \hat{\mathbf{k}} \cdot \hat{\mathbf{r}} \hat{\mathbf{k}}$ . The real part of the potential generates a phase shift, whereas the imaginary part represents a loss of flux. As we shall see below, both factors can significantly modify the correlation function.

With the distorted single particle amplitude  $\varphi_k(x) = e^{ik \cdot x} g(\mathbf{k}, \mathbf{r})$  as per Eq. (16), the two-pion correlation function, Eq. (11), becomes

$$C_2(\mathbf{k}_1, \mathbf{k}_2) = 1 + |f(\mathbf{k}_1, \mathbf{k}_2)|^2. \quad (17)$$

The second term, generated by the interference of the two distorted waves, is given by the square modulus of the overlap integral

$$f(\mathbf{k}_1, \mathbf{k}_2) = \frac{1}{N} \int d^3r \rho(\mathbf{r}) g(\mathbf{k}_1, \mathbf{r}) g(\mathbf{k}_2, \mathbf{r}) e^{i\mathbf{q} \cdot \mathbf{r}}, \quad (18)$$

where  $N = \int d^3r \rho(\mathbf{r}) g(\mathbf{k}, \mathbf{r})$ . In the absence of pion–source–medium interactions, so that  $g(\mathbf{k}, \mathbf{r}) = 1$ , the integral is reduced to the Fourier transform of the source distribution  $\rho(\mathbf{r})$ . In this limit we thus recover the familiar result that the correlation function depends only on  $\mathbf{q} \equiv \mathbf{k}_1 - \mathbf{k}_2$ . In general, however,  $f(\mathbf{k}_1, \mathbf{k}_2)$  depends on the relative angle  $\phi$  of the two momenta  $\mathbf{k}_1$  and  $\mathbf{k}_2$ ; hence, the correlation function also has this dependence.

In Sec. III, we present numerical results for a finite, complex optical potential. However, a discussion of the black sphere limit ( $\sigma_I \rightarrow -\infty$ ,  $\rho(r) = \rho_o \theta(R - r)$ ) serves as a useful illustration of the physics involved. Under these circumstances the outgoing pion amplitude attenuates to zero when its classical path transits the potential region. On the other hand, the source distribution  $\rho(r)$  is zero for  $r > R$ . We shall assume that the pions are emitted in a thin spherical shell of width  $\delta$  outside  $R$  and then compute the  $\delta \rightarrow 0$  limit. The distortion factor  $g(\mathbf{k}, \mathbf{r})$  is determined purely by geometry:

$$g(\mathbf{k}, \mathbf{r}) = \theta \left( \hat{\mathbf{k}} \cdot \hat{\mathbf{r}} + \sqrt{1 - \frac{R^2}{r^2}} \right) \theta(r - R). \quad (19)$$

Equation (18) thus reduces to

$$f(\mathbf{k}_1, \mathbf{k}_2) = \frac{1}{2\pi} \int d\Omega \theta(\hat{\mathbf{k}}_1 \cdot \hat{\mathbf{r}}) \theta(\hat{\mathbf{k}}_2 \cdot \hat{\mathbf{r}}) e^{i\mathbf{q} \cdot \mathbf{R}}. \quad (20)$$

The resulting correlation function can be evaluated numerically for general  $\phi$ . It can also be calculated analytically in the following two cases. For parallel pions, so that  $\phi = 0$ ,  $f$  becomes

$$f(\mathbf{k}_1, \mathbf{k}_2) = \frac{1}{iqR} [e^{iqR} - 1] , \quad (21)$$

so that

$$C_2(\mathbf{k}_1, \mathbf{k}_2) = 1 + \frac{4}{q^2 R^2} \sin^2 \left( \frac{qR}{2} \right) . \quad (22)$$

In this case, the correlation function is simply a function of the dimensionless quantity  $qR$ , where  $q \equiv |\mathbf{q}|$  is the magnitude of the relative 3-momentum of the two pions. However, for pions emitted back-to-back, so that  $\phi = \pi$ ,  $f$  vanishes. Thus,  $C_2(\mathbf{k}_1, \mathbf{k}_2)|_{\hat{\mathbf{k}}_2 = -\hat{\mathbf{k}}_1} = 1$  for all  $q$ . The attenuation of the emission amplitude which penetrates the absorbing region destroys the interference entirely.

The physical origin of the  $\phi$  dependence can be readily understood in this limit and is illustrated in Figs. 1 and 2. For parallel pairs the deviation of the correlation function from unity is caused by the constructive interference of the two amplitudes corresponding to Figs. 1a and 1b. However, for antiparallel pairs, the amplitude for the process in Fig. 2b, which would interfere with the amplitude in Fig. 2a, is completely suppressed by absorption in the source region; hence, in this case there is no enhancement.

We can now proceed to evaluate Eq. (20) for arbitrary  $\phi$  and total pion momentum  $P \equiv |\mathbf{k}_1 + \mathbf{k}_2|$ . For given  $P$  and  $\phi$ , there is a minimum  $q$  allowed kinematically; that is,

$$q_{\min} = P \left( \frac{1 - \cos \phi}{1 + \cos \phi} \right)^{1/2} . \quad (23)$$

As  $\phi$  increases,  $q_{\min}$  becomes non-negligible. At large opening angles,  $q_{\min}$  is large, and only a small correlation between the pions remains — regardless of any pion–source–medium interactions. We therefore consider small opening angles, where  $q_{\min}$  is small, so that the suppression of the correlation due to interactions with the source medium is easily detectable.

In Fig. 3, we show the correlation function for several  $\phi$  at two fixed values of  $PR$  in the above black sphere limit. As shown in Eq. (22), the correlation function of parallel pairs goes to two at zero  $q$ . For comparison, the solid line shows the correlation function which results from ignoring final-state interactions. That is,  $g(\mathbf{k}, \mathbf{r})$  is set to unity in Eq. (18), and a uniform, spherical source of radius  $R$  is assumed, so that

$$C_2^{\text{free}}(qR) = 1 + \left[ \frac{3(\sin qR - qR \cos qR)}{(qR)^3} \right]^2 . \quad (24)$$

The two correlation functions are independent of  $\phi$  and  $P$ , yet the scales with which they fall off in  $qR$  are different. In the *black* sphere case the correlation of parallel pairs at intermediate  $q$  is *enhanced*. This result can be understood physically as follows: when the source region is black, only pion pairs emitted from the front surface — as shown in Fig. 1 — are detected; the pairs emitted from opposite sides as illustrated in Fig. 4 are suppressed. The effective source size is thus *smaller* than it would be if all the pairs were sampled, leading to an enhanced correlation at intermediate  $q$ . When the opening angle between the pions becomes non-zero, the correlation function is suppressed relative to the parallel pion case, due to the final-state interactions. For  $PR = 10$  (20), corresponding to  $P \approx 400$  (800) MeV

for a source radius of  $R \approx 5$  fm, Fig. 3 shows the suppression of the correlation function as  $\phi$  increases from  $0^\circ$  (dashed line) to  $5^\circ$  (crosses),  $10^\circ$  (squares), and  $20^\circ$  (pluses).

Based on the above discussion, we hypothesize that these absorption effects should be quite general and thus present in fermion interferometry as well.

#### IV. NUMERICAL RESULTS AND PHENOMENOLOGICAL CONSEQUENCES

In this section we compute the correlation function ratio, Eq. (11), for the finite, complex optical potential of Eq. (15). For illustrative purposes, we choose simple forms for the source density  $\rho(r)$ , a Gaussian  $\rho(r) = \rho_o \exp(-r^2/R_G^2)$  and a uniform sphere  $\rho(r) = \rho_o \theta(R_S - r)$ , with  $R_S = \sqrt{2.5}R_G$ . The density parameters are chosen so that the two source functions have the same rms radii and central densities. Note that the integral  $\int d^3r \rho(r)$  differs in the two densities chosen. We equate the central densities of the two sources, rather than the number of particles  $\int d^3r \rho(r)$  they contain, as we believe the central density better characterizes the heavy ion collision. We presume that the fireball resulting from the heavy-ion collision is baryon-rich for simplicity, as is the case for heavy ion experiments in the nuclear stopping regime, such as those at the AGS [17,18]. We thus choose  $\rho_o = 0.17 \text{ fm}^{-3}$ .

Given  $\rho(r)$ , we need to estimate the constants  $\sigma_R$  and  $\sigma_I$ . In our treatment of  $U(x)$ ,  $\sigma_R$  and  $\sigma_I$  are proportional to the effective, forward  $\pi N$  scattering amplitude in the fireball. The  $\pi N$  amplitude in free space is well-known [19]: due to 3-3 resonance formation, the imaginary part of the amplitude has a large peak near a pion laboratory energy of 200 MeV, around which the real part changes the sign. Below and above this energy region, the amplitude varies less and is of smaller magnitude. It involves many  $\pi N$  resonances at higher energies.

The construction of an effective  $\pi N$  amplitude in nuclei from the free-space amplitude is an involved procedure, but the issues are well understood [20]. The main issues involved in its construction are as follows. 1)  $\Delta$  resonance formation depends on the *local* relative momentum of the  $\pi - N$  system, so that in the medium a minimally non-local optical potential is required. 2) Nuclear pion absorption involves more than one nucleon, so that the nucleon correlations in the medium become important. 3) Higher-order scattering contributions are now possible as well, and these also involve nucleon correlations. In view of the uncertainties in averaging over the initial source states and summing over the final states in constructing the potential in the fireball, we assume that these complications can be effectively included by varying the parameter values in our local potential.

Since we use a simple model to illustrate the essential physics that emerge, we first choose a representative parameter set for  $\sigma_R$  and  $\sigma_I$  and vary it over a wide range. The representative set is based on 1) the free-space  $\pi N$  scattering amplitude, taking into account 2) nuclear pion absorption and 3) the non-observation of the initial and final states of the pion source, which acts to increase the pion's effective mean-free path [21,22]. We assume that the form of Eqs. (11) and (12) is preserved under the inclusion of this last effect, yet this need not be so. Finally, the representative set we choose is  $(\sigma_R, \sigma_I) = (\pm 2, -2) \text{ fm}^2$ , which corresponds to a characteristic absorption length of  $(\sigma \rho_o)^{-1} = 1.5 \text{ fm}$  in nuclear matter. In order to explore a wider range of parameter values, we multiply this reference value by a scale factor  $c$  such that  $(\sigma_R, \sigma_I) = (\pm 2, -2)c \text{ fm}^2$  and vary  $c$ . To ensure that our examination is



not prejudiced by our choice of the imaginary to real ratio, we also examine the cases  $\sigma_R = 0$  and  $\sigma_I = 0$ .

In general, the correlation function depends on the kinematics of the pion pair —  $\mathbf{k}_1, \mathbf{k}_2$  — as well as on the parameters characterizing the source —  $R, \sigma_R, \sigma_I$ . For a spherically symmetric source, if final-state interactions are ignored, the correlation function depends only on  $q$  and  $R$ . However, if  $U \neq 0$ , it depends on the opening angle  $\phi$  and the total pair momentum  $P$  as well. In this section, we discuss these new dependences in turn.

As discussed previously, we expect the correlation function to be suppressed at large opening angles as a consequence of including absorption in the source region. Our calculations with a finite optical potential show that to be indeed the case. In Fig. 5 we plot the opening angle dependence of the correlation function at  $P = 400$  MeV and  $q = 40$  MeV for both a uniform source of  $R_S = 10$  fm and a Gaussian source of  $R_G = 5$  fm. The  $c = 0$  results — here there are no final-state interactions — do not depend on  $\phi$ , yet there is always a significant suppression of  $C_2$  as  $\phi$  increases for finite  $\sigma_I$ , in qualitative agreement with the black sphere results. We observe the same behavior if we fix  $\sigma_I$  and vary  $\sigma_R$ , or vice versa, rather than varying them together. To wit, *absorption by the source leads to suppression of the correlation at finite opening angles.*

If one averages the correlation function over the opening angle, the results turn out to be rather insensitive to  $P$ . We therefore fix  $P$  and investigate the sensitivity of the opening-angle-averaged  $C_2$  to the optical potential. The range of  $\phi$  is restricted kinematically:

$$\phi < \arccos \left[ \frac{P^2 - q^2}{P^2 + q^2} \right]. \quad (25)$$

Thus, for fixed  $P$ , as  $q$  increases, one includes an ever larger proportion of large opening angle pairs in  $C_2$ , the correlation of which are suppressed. Angle-averaging thus results in a rather reduced correlation in the intermediate and large  $q$  range. At the lowest  $q$ , only parallel pairs are included, and the correlation approaches the Bose-Einstein limit,  $C_2 = 2$ , as  $q \rightarrow 0$ , producing a non-Gaussian shape in the low  $q$  region. If one fits a standard Gaussian form to the correlation function,

$$C_2 = 1 + \lambda \exp \left[ -q^2 R_e^2 \right], \quad (26)$$

as is done with experimental data [17], to extract the effective source size  $R_e$  and the “coherence parameter”  $\lambda$ , one finds a smaller effective source size  $R_e < R$  and  $\lambda < 1$ . The absorption of pions in the source region therefore leads to a small effective  $R_e$  and  $\lambda$ , as well as to a non-Gaussian shape of the correlation function in the low  $q$  region.

In Fig. 6 we show the opening-angle-averaged correlation functions for both sources with several values of  $c$ . Note that  $P = 400$  MeV and  $R = 10(5)$  fm for the uniform (Gaussian) source. For each source, we show the results for both signs of  $\sigma_R$ . Three curves are shown in each panel corresponding to  $c = 0$  (dashed lines), 1 (solid lines), and 10 (dot-dash lines). These results indicate a small but significant change in the shape of the correlation functions once the final-state interactions are turned on. Indeed, the medium-modified correlation function displays a non-Gaussian shape, especially at low  $q$ , even for a Gaussian source.

Such non-Gaussian correlation functions have been seen [17,18,23]. For comparison, we show the E802 data for the  $\pi^-$  correlations in  $14.6A$  GeV/c  $^{28}\text{Si} + ^{197}\text{Au}$  collisions [18]

together with our calculation in Fig. 7. The data can be fit to the form in Eq. (26) with  $R_e = 3.42 \pm 0.26$  fm and  $\lambda = 0.65 \pm 0.07$ , yet the static Gaussian model we use also reproduces the correlation function if one assumes  $R_G \approx 5$  fm and  $c \neq 0$ . The solid line in the figure is calculated assuming  $P = 400$  MeV and  $c = 10$ . The results for  $P = 600$  MeV are almost identical. The agreement with data can be improved if we vary both the optical potential and  $R_G$ . However, our goal here is not a quantitative fit to the data — especially in light of our simple assumptions regarding the static source and its interaction — but, rather, a qualitative insight into how non-Gaussian shapes can be generated. Note that Fig. 7 also suggests that a study of the opening-angle dependence may be a better way to infer the extent of pion–source–medium interactions.

If  $|\sigma_I|$  is small, one may be able to detect the correlation effects induced by the real part of the optical potential. The extra phase introduced by the final-state interaction,  $\exp(-i\sigma_R t)$ , modifies each of the pion wavefunctions and leads to an interference pattern in the correlation function. Such effects can be seen most clearly if a sharp edge is present in the source and the damping factor  $\exp(-|\sigma_I|t)$  is small. In Fig. 8, we show the  $\phi$ -averaged correlation functions for a uniform spherical source with several values of  $\sigma_R$  and two values of  $\sigma_I$ . A large oscillation is observed in Fig. 8a when  $\sigma_I = 0$  and  $\sigma_R$  is of roughly  $-1.5$  fm<sup>2</sup>. The correlation function becomes as large as 4.5 at  $q = 100$  MeV! Note, however, that we have not excluded bound-state forming parameters for  $\sigma_R < 0$  and small  $\sigma_I$ . The oscillations damp out quickly as  $\sigma_I$  grows large, as shown in Fig. 8b.

At fixed  $P$ ,  $q$ , and  $R$ , one can compare the values of  $C_2$  for different  $\sigma_R$  and  $\sigma_I$ . Fig. 9a shows the variations of  $C_2$  with respect to  $\sigma_R$ , for various fixed  $\sigma_I$ . In the upper panel,  $\sigma_I = 0$ , whereas  $\sigma_I = -2$  and  $-4$  fm<sup>2</sup> — the solid and dashed lines, respectively — in the lower panel. The interference pattern is clearly seen at  $\sigma_I = 0$ , yet only a small variation is observed for a more realistic value of  $\sigma_I$ . Note, however, the sudden jump in  $C_2$  when  $\sigma_R$  changes sign. Similarly, we study  $C_2$  as a function of  $\sigma_I$  for various  $\sigma_R$  in Fig. 9b. That is, we choose  $\sigma_R = \pm 2$  fm<sup>2</sup> — the dashed and solid lines — and 0 — the dot-dashed line. The interference induced by  $\sigma_R$  enhances or suppresses the correlation for  $\sigma_R < 0$  or  $\sigma_R > 0$  if  $|\sigma_I|$  is less than about 2 fm<sup>2</sup>.

Even though our model is currently too simple to take its comparison with experiment seriously, the generation of modifications to the correlation function’s shape by the pion–source–medium interaction is significant and robust. From our model the following simple picture emerges: the inclusion of pion–source–medium interactions leads to 1) a suppression of the correlation as the opening angle increases, 2) an angle-averaged correlation function which can deviate from a Gaussian shape at low  $q$ , as well as 3) possible additional interference effects from the real part of the potential. The last effect is suppressed by the inclusion of absorption, and when  $\sigma_I$  exceeds or is of the order of the value in normal nuclear matter the correlation becomes insensitive to the real part. If one fits the correlation data with a simple Gaussian form, Eq. (26), these effects will lead to a small *apparent* source radius and a small coherence parameter,  $\lambda < 1$ .

## V. CONCLUSIONS

Using a simple model for the pion–source–medium interaction, in the eikonal approximation, we have demonstrated that an interesting momentum dependence in the two-pion

momentum correlation function is generated. Specifically, when absorptive interactions are finite, the pion correlation function decreases rapidly as the opening angle between the pions increases. Our model is a simple one, yet this behavior should not be sensitive to the assumptions we have made. Pion-interferometry analyses have usually been performed as a function of only two of the two-pion momentum variables, implicitly assuming that the correlation function is independent of the opening angle. Our discovery of a strong opening-angle dependence thus suggests that analyses should be carried out explicitly in terms of the opening angle as well. Note, moreover, that the opening-angle-averaged pion correlation function exhibits a non-Gaussian shape when pion–source-medium interactions are included, even for a Gaussian source. This provides an alternative explanation for the coherence factor  $\lambda$ , which is usually invoked to fit experimental data.

### ACKNOWLEDGMENTS

We thank S. E. Koonin and M. Gyulassy for stimulating discussions, and M. Macfarlane and B. Serot for comments on the manuscript. This research is supported in part by the U. S. National Science Foundation, Grants No. PHY90-13248 and PHY91-15574, at Caltech, by the U.S. Department of Energy, Grant No. DE-FG02-87ER40365 at Indiana University and Grant No. DE-FG03-87ER40347 at California State University, Northridge, and by the Grant-in-Aid for Scientific Research, Japan Ministry of Education and Culture, No. C06640394.

## REFERENCES

- [1] R. Hanbury-Brown and R. Q. Twiss, *Phil. Mag.* **45**, 663 (1954).
- [2] G. Goldhaber, S. Goldhaber, W. Lee, and A. Pais, *Phys. Rev.* **120**, 300 (1960).
- [3] G. I. Kopylov and M. J. Podogoretsky, *Yad. Fiz.* **15**, 392 (1972) [*Sov. J. Nucl. Phys.* **15**, 219 (1972)]; *Yad. Fiz.* **18**, 656 (1973) [*Sov. J. Nucl. Phys.* **18**, 336 (1974)].
- [4] E. V. Shuryak, *Phys. Lett.* **44B**, 387 (1973).
- [5] F. B. Yano and S. E. Koonin, *Phys. Lett.* **B78**, 556 (1978).
- [6] M. Gyulassy, S. K. Kauffmann, and L. W. Wilson, *Phys. Rev. C* **20**, 2267 (1979).
- [7] S. Pratt, *Phys. Rev. Lett.* **53**, 1219 (1984).
- [8] W. Bauer, C. -K. Gelbke, and S. Pratt, *Ann. Rev. Nucl. Part. Sci.* **42**, 77 (1992) and references therein.
- [9] G. Bertsch, M. Gong, L. McLerran, V. Ruuskanen, and E. Sarkkinen, *Phys. Rev. D* **37**, 1202 (1988).
- [10] S. S. Padula, M. Gyulassy, and S. Gavin, *Nucl. Phys.* **B329**, 357 (1990).
- [11] K. S. Lee, E. Schnedermann, J. Sollfrank, and U. Heinz, *Nucl. Phys.* **A525**, C523 (1991).
- [12] M. Gyulassy and S. S. Padula, *Phys. Lett.* **B217**, 181 (1988).
- [13] G. F. Bertsch, P. Danielewicz, and M. Herrmann, *Phys. Rev. C* **49**, 442 (1994).
- [14] S. Pratt, P. Siemens and A. P. Vischer, *Phys. Rev. Lett.* **68**, 1109 (1992).
- [15] M. Gyulassy, *Phys. Rev. Lett.* **48**, 454 (1982).
- [16] C. Smit, *Lett. Nuovo Cimento* **4**, 454 (1970); C. Wilkin, *Lett. Nuovo Cimento* **4**, 491 (1970); A. T. Hess and J. M. Eisenberg, *Phys. Lett.* **47B**, 311 (1973).
- [17] See for example, H. Beker *et al.*, *Nucl. Phys.* **A566**, 115c (1994), and references therein; Nu Xu, *Nucl. Phys.* **A566**, 585c (1994).
- [18] T. Abbott *et al.*, *Phys. Rev. Lett.* **69**, 1030 (1992).
- [19] Particle Data Group, *Phys. Rev. D* **45**, S1 (1992).
- [20] J. M. Eisenberg and D. S. Koltun, *Theory of Meson Interactions with Nuclei* (John Wiley & Sons, New York, 1980); T. Ericson and W. Weise, *Pions and Nuclei* (Clarendon Press, Oxford, 1988).
- [21] R. J. Glauber, in *Lectures in Theoretical Physics*, edited by W. E. Brittin and L. G. Dunham (Interscience, New York, 1959), Vol. I, p. 315.
- [22] A. Kohama, K. Yazaki, and R. Seki, *Nucl. Phys.* **A536**, 716 (1992); *ibid* **A551**, 687 (1993).
- [23] M. R. Adams *et al.*, *Phys. Lett.* **B308**, 418 (1993).

## FIGURES

FIG. 1. Emission of a parallel pair of pions from the source region. The amplitude in a) interferes constructively with the exchange amplitude in b).

FIG. 2. Emission of an anti-parallel pair of pions from the source region. The amplitude in a) would interfere constructively with the exchange amplitude in b), but the latter is suppressed by absorption in the source region.

FIG. 3. Two-particle correlation from a black sphere source of radius  $R$  as a function of the relative momentum  $q = |\mathbf{k}_1 - \mathbf{k}_2|$ . The total momentum  $P = |\mathbf{k}_1 + \mathbf{k}_2|$  is  $10/R$  in a) and  $20/R$  in b). The solid lines indicate the results with no pion–source-medium interactions. The source region is assumed to be spherical and uniform. When the source medium is absorptive, the correlation function also depends on the opening angle  $\phi$  between the particles. Shown are the results for  $\phi = 0^\circ$  (dashed lines),  $5^\circ$  (crosses),  $10^\circ$  (squares), and  $20^\circ$  (pluses). For fixed  $P$  and  $\phi$ , there is a minimum  $q$ , Eq. (23), allowed kinematically.

FIG. 4. Emission of a parallel pair of particles from opposite sides of the source region. This process is suppressed compared to the emission in Fig. 1 if the source region is absorptive.

FIG. 5. Two-pion correlation as a function of the opening angle  $\phi$  between the particles. The relative momentum is fixed at  $q = 40$  MeV, and the total momentum at  $P = 400$  MeV. The optical potential is chosen with  $(\sigma_R, \sigma_I) = (\pm 2, -2)c$  fm<sup>2</sup>, and the results are shown here for a range of  $c$ . If the final-state interaction is ignored, so that  $c = 0$ ,  $C_2$  does not depend on  $\phi$ , as indicated by the solid lines. When absorption is present, the correlation decreases as  $\phi$  increases. Note that  $c = 1, 10$  correspond to the dashed and the dot-dashed lines, respectively. Results for both a uniform sphere of radius  $R_S = 10$  fm, in a) and c), and a Gaussian source of  $R_G = 5$  fm, in b) and d), are shown with both signs of  $\sigma_R$ .

FIG. 6. Two-pion correlation function averaged over the pions' opening angle, as a function of  $q$ . The total pion momentum is  $P = 400$  MeV. Results for three different final-state interactions are shown, and, as in Fig. 5,  $c = 0, 1, 10$  correspond to the dashed, solid, and dot-dashed lines, respectively.

FIG. 7. Comparison of the pion correlation function calculated using a static Gaussian source model ( $R_G = 5$  fm) and the E802 data, corrected for acceptance and Coulomb effects, for the  $\pi^-$  correlation in  $14.6A$  GeV/ $c$   $^{28}\text{Si} + ^{197}\text{Au}$  collisions [18] with  $q$ . The solid line indicates the results using  $\sigma = -20 - 20i$  fm<sup>2</sup> ( $c = 10$ ), whereas the dashed line represents the non-interacting ( $c = 0$ ) results. In our calculation  $P = 400$  MeV, but the results are insensitive to  $P$ .

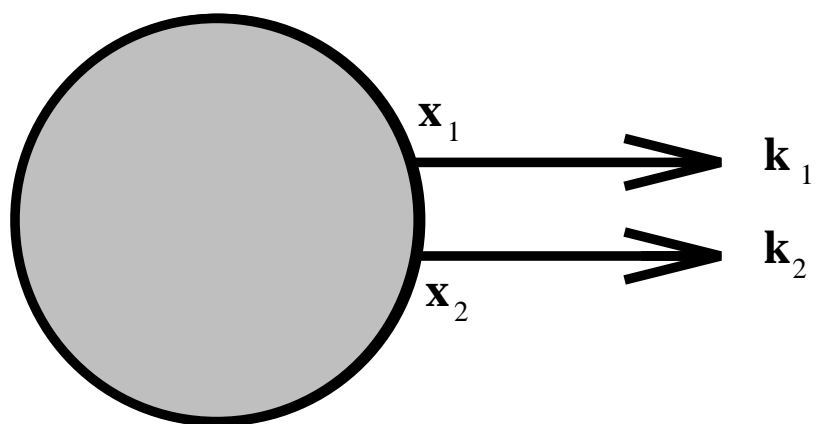
FIG. 8. Opening-angle-averaged pion correlation function as a function of  $q$  for various  $\sigma_R$  and a uniform spherical source of  $R_S = 10$  fm.  $P$  is fixed at 400 MeV, and in a)  $\sigma_I = 0$ , whereas in b)  $\sigma_I = -2$  fm<sup>2</sup>. The curves correspond to different values of  $\sigma_R$ ; that is, the results with  $\sigma_R = -3$ ,  $-1.5$ ,  $0$ , and  $3$  fm<sup>2</sup> are denoted by dashed, dot-dashed, solid, and dotted lines, respectively. A large oscillation is seen for  $\sigma_R \sim -1.5$  fm<sup>2</sup> if  $\sigma_I = 0$ , but very little sensitivity to  $\sigma_R$  is observed for more realistic  $\sigma_I$ .

FIG. 9. Dependence of the opening-angle-averaged pion correlation function on a)  $\sigma_R$  and b)  $\sigma_I$ . The calculation is performed with  $P = 400$  MeV and  $q = 40$  MeV for a uniform spherical source of  $R_S = 10$  fm. In a), the upper panel shows the results for  $\sigma_I = 0$ , whereas the lower panel shows those for  $\sigma_I = -2$  and  $-4$  fm<sup>2</sup> — the solid and dashed lines, respectively. In b), the results for  $\sigma_R = -2$ ,  $0$ ,  $2$  fm<sup>2</sup> are denoted by solid, dot-dashed, and dashed lines. The oscillations seen in Fig. 8 give rise to a large modification of the correlation at small  $|\sigma_I|$ .

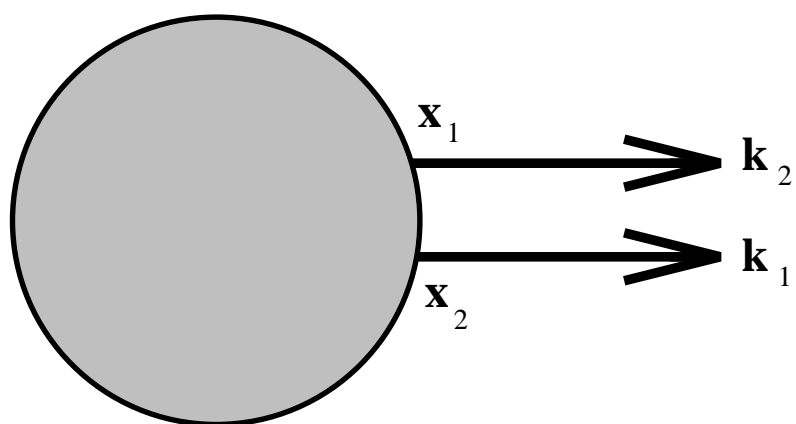
This figure "fig1-1.png" is available in "png" format from:

<http://arxiv.org/ps/nucl-th/9408005v1>

a)



b)





This figure "fig2-1.png" is available in "png" format from:

<http://arxiv.org/ps/nucl-th/9408005v1>

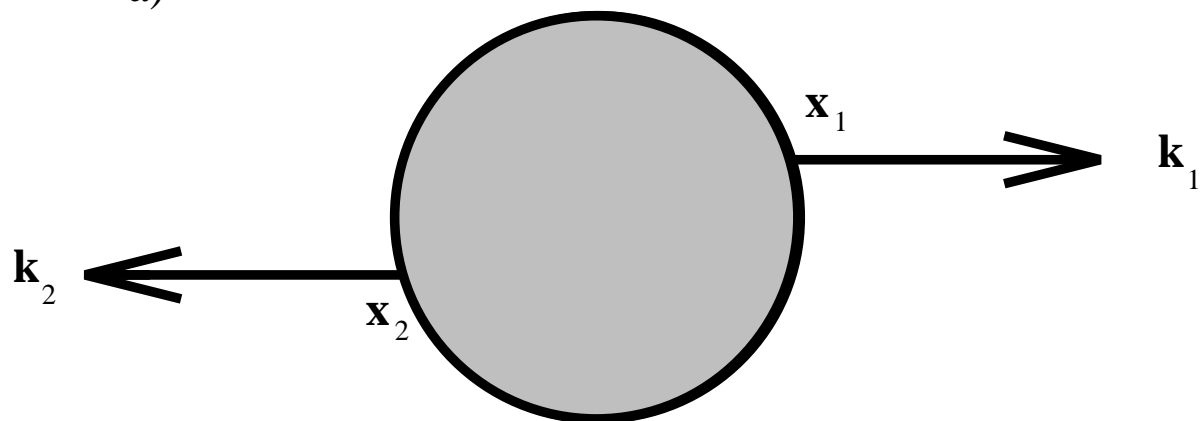
This figure "fig1-2.png" is available in "png" format from:

<http://arxiv.org/ps/nucl-th/9408005v1>

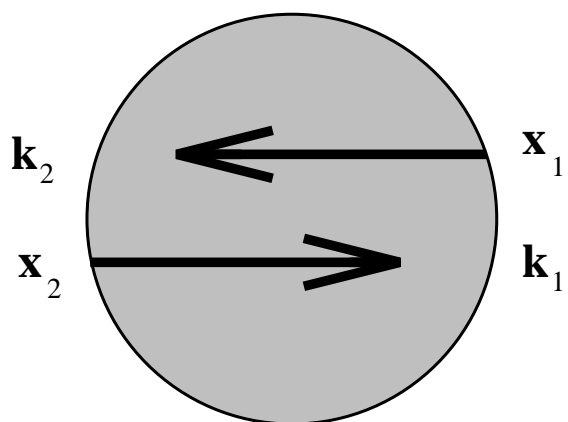
This figure "fig2-2.png" is available in "png" format from:

<http://arxiv.org/ps/nucl-th/9408005v1>

a)



b)

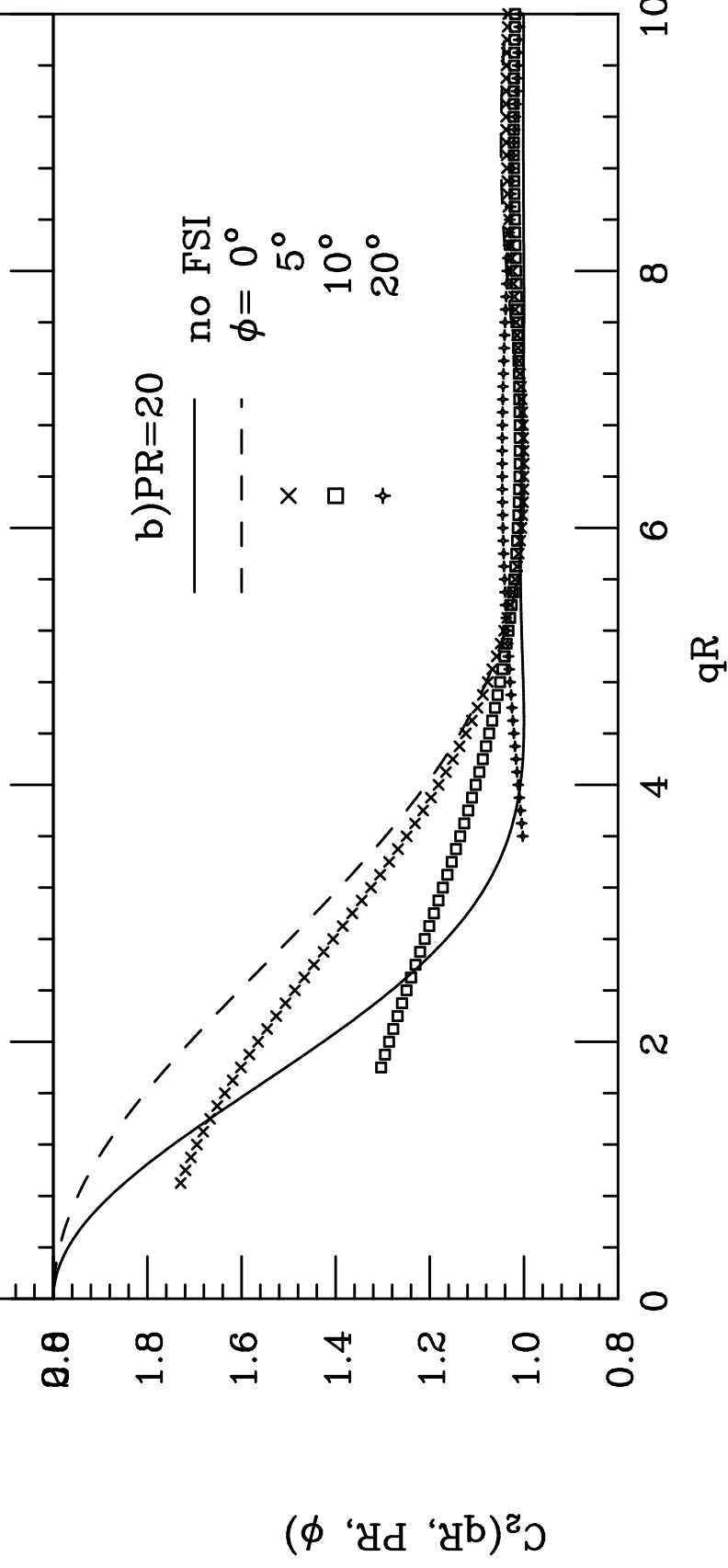
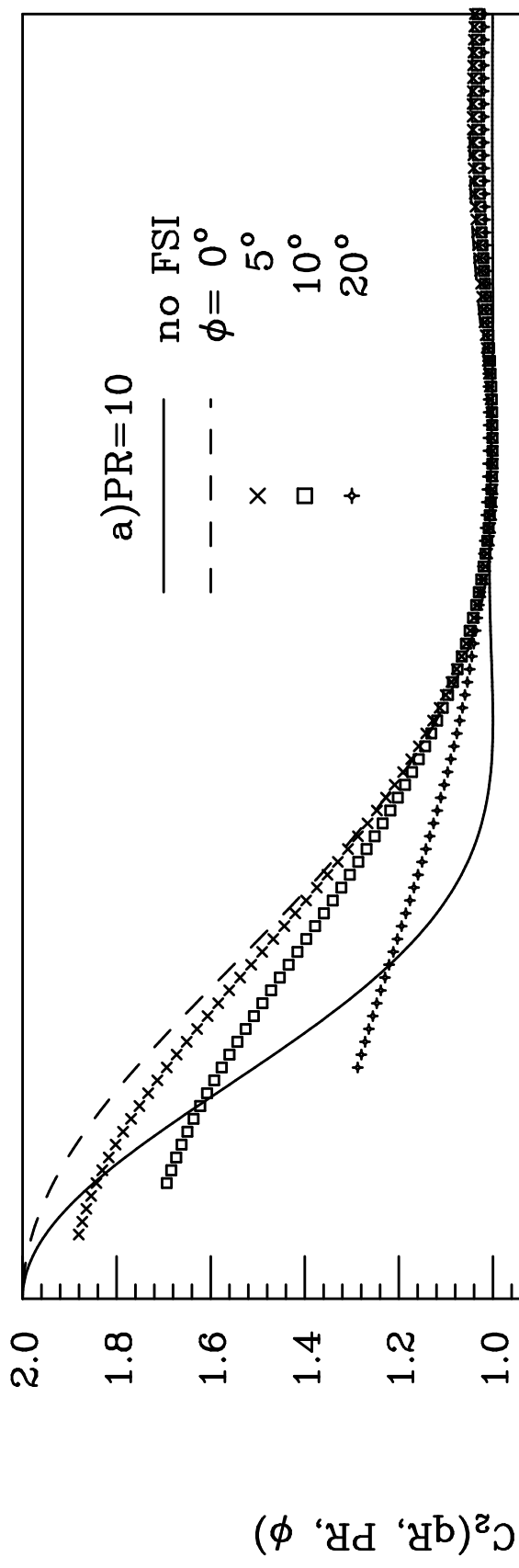


This figure "fig1-3.png" is available in "png" format from:

<http://arxiv.org/ps/nucl-th/9408005v1>

This figure "fig2-3.png" is available in "png" format from:

<http://arxiv.org/ps/nucl-th/9408005v1>



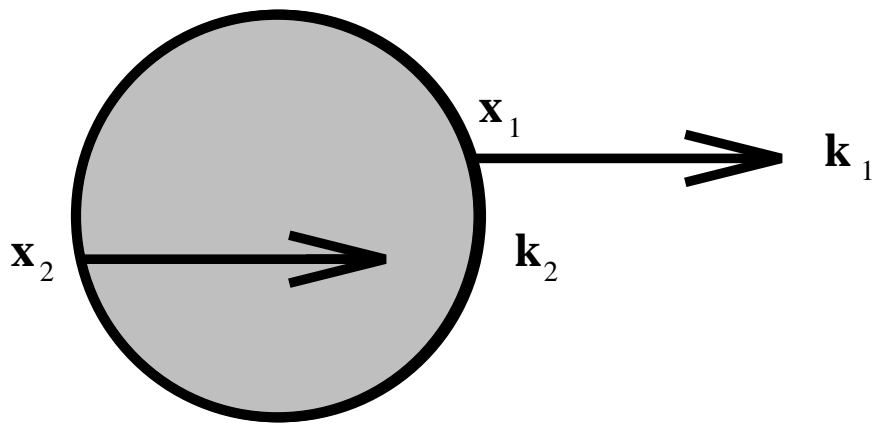
This figure "fig1-4.png" is available in "png" format from:

<http://arxiv.org/ps/nucl-th/9408005v1>



This figure "fig2-4.png" is available in "png" format from:

<http://arxiv.org/ps/nucl-th/9408005v1>



+ exchange

This figure "fig1-5.png" is available in "png" format from:

<http://arxiv.org/ps/nucl-th/9408005v1>

